ICARUS **120,** 106–118 (1996)
ARTICLE NO. 40

Collisional and Dynamical History of Ida

RICHARD GREENBERG, WILLIAM F. BOTTKE, MICHAEL NOLAN,[1] PAUL GEISSLER, JEAN-MARC PETIT,[2] AND DANIEL D. DURDA

Lunar and Planetary Laboratory, University of Arizona, Tucson, Arizona 85721
E-mail: greenberg@lpl.arizona.edu

ERIK ASPHAUG

NASA Ames Research Center, Moffett Field, California 94035

AND

JAMES HEAD

Brown University, Providence, Rhode Island 02912

Received April 3, 1995; revised July 24, 1995

The history of Ida is constrained by its membership in the Koronis family, its satellite Dactyl, the record of impacts left on its surface, and other dynamical, morphological, and spectral properties. Models of crater production and comparably effective erasure processes, combined with the current size–frequency distribution of craters, suggest that the age of the surface is either about 50 myr or >1 byr. The younger age may be inconsistent with the degraded appearance of many craters, while the older age conflicts with the collisional life expectancy of Dactyl. Consideration of Dactyl's evolution may resolve this issue as well as shed light on the formation of Dactyl, the density of Ida, and possible source regions for Ida and Dactyl within the Koronis parent body.

I. INTRODUCTION

Like the asteroid 951 Gaspra, the asteroid 243 Ida, more recently imaged by the Galileo spacecraft (Belton *et al.* 1994), formed and evolved under the overwhelming influence of collisional processes. Interpretation of the earlier images of Gaspra, based on theoretical models of the results of impacts on such an irregular small body (18 km in length), revealed new results regarding the collisional environment around Gaspra, and the nature of the response of Gaspra to impacts (Greenberg *et al*. 1994). For example, the impacting population was found to have a surprisingly steep size distribution, and global jolting by large impacts modifies the cratering record by frequently erasing smaller craters over the entire surface. Ida differs from Gaspra in a number of fundamental ways, both in its observable physical properties and in its setting among impacting populations of smaller bodies. The challenge to interpreters is to develop a scenario for the history of Ida that accounts for its differences from Gaspra, while invoking a consistent physical model.

The following differences provide critical constraints in developing such a scenario:

(a) Ida is much larger than Gaspra (about 56 km long), and even more elongated and irregular in shape (Belton *et al*. 1994). Impactors of a given size are likely to produce different sized craters on Ida than on Gaspra, and to have different ancillary effects such as jolting other portions of the surface (Greenberg *et al.* 1994). The irregular shape suggests for Ida (and maybe even for Gaspra) a global structure of large solid blocks underlying rubble and regolith.

(b) Ida is a member of a dynamical family, the prominent Koronis family, while Gaspra is not. Family membership places constraints on Ida's formation and lifetime: According to an estimate of the time for collisions to erode and diffuse the Koronis family so that it would be indistinguishable from the background population, the family must be less than about 1.5 byr old (Durda 1993). A similar result (<2 byr) has been obtained by Marzari *et al*. (1995). Observed rotation rates suggest an age limit of <4 byr (Binzel 1988, although that result is referenced as <1 byr by Belton *et al.* 1994), so Durda's estimate of <1.5 byr

[1] Current address for M. C. Nolan: Arecibo Observatory, PO Box 995, Arecibo, PR 00613.

[2] Permanent address for J.-M. Petit: Observatoire de Nice, B.P. 139, F-06003 Nice, France.

0019-1035/96 $18.00

stands as the strongest constraint independent of the Ida images. The family probably does not contribute significantly to the total population impacting Ida (Bottke *et al.* 1994), unless the family has a grossly disproportionate number of members too small to see (Zappalà and Cellino 1994).

(c) Ida has a satellite, Dactyl, whose existence places specific constraints on the collisional history of Ida. A process, such as an impact event, by which Dactyl was liberated from Ida and placed into orbit is implausible. More likely, Dactyl is a primordial companion, bound to Ida since the disruption of their common source, the Koronis parent body (Durda 1994). An object of Dactyl's size is unlikely to survive impact disruption for more than 10^8 yr, which is at odds with some estimates of the age of Ida ($\sim$1 byr according to Belton *et al.* 1994) based on a preliminary interpretation of the crater statistics. Due to the shape and rotation of Ida, the observed orbit of Dactyl is unstable on time-scales <1 yr unless the mass density of Ida is well below 3 g/cm^3 (Petit *et al.* 1994, Belton *et al.* 1995).

(d) Ida is located closer to the center of the main belt, so approximately 40% more asteroids cross its orbit than cross Gaspra's. The impact frequency is probably proportionately higher, assuming that the observable larger asteroids provide a measure of the relative numbers of small impactors (Bottke *et al.* 1994).

(e) Because Ida's orbital eccentricity and inclination are unusually small relative to most main-belt asteroids, impact velocities are generally low on Ida. The average value is 3.55 km/sec, compared with 5.0 km/sec for Gaspra (Bottke *et al.* 1994).

(f) The size distribution of craters is markedly different on Ida compared with Gaspra. The area density of all craters with diameter larger than 200 m is similar on both bodies, but there are five times as many craters (per unit area) larger than 1 km on Ida as on Gaspra (Belton *et al.* 1994).

(g) Large concavities on Ida, with dimensions comparable to those of the asteroid (several nearly 10 km in diameter or larger), have the appearance of impact craters, albeit with somewhat unusual morphologies (Asphaug *et al.* 1996). Proportionately large concavities on Gaspra appear very different from familiar craters, but may well be craters nonetheless (Greenberg *et al.* 1994). For craters larger than 3 km, we count a similar number per unit area on Ida to the estimate for Gaspra by Greenberg *et al.* (1994). On Ida the largest craters (4–10 km diameter) follow approximately the same power-law size distribution as smaller craters, while on Gaspra the largest ones (1–4 km) are overabundant relative to an extrapolated power law.

(h) Ida is one of the fastest rotators among known asteroids (Lagerkvist *et al.* 1989), with a period of only 4.63 hr. Combined with Ida's elongated and irregular shape, this rotation yields a complex dynamical environment that can have significant effects on the transport and distribution of impact-derived ejecta (Geissler *et al.* 1996). These dynamical effects can affect the observed spatial distribution of boulders over the surface of Ida (Geissler *et al.* 1994a,b) and the range of stable orbits of Ida's moon (Petit *et al.* 1994), as well as the transport of ejecta between Dactyl and Ida (Geissler *et al.* 1994c).

In this paper we develop a scenario for the impact history of Ida that fits the above observational constraints. Our scenario invokes the same impacting-population size distribution as was implied by the Gaspra analysis by Greenberg *et al.* (1994). We model the same impact processes of crater formation and of crater removal as in the Gaspra model, with scaling appropriate to the size of Ida based on hydrocode simulations of impacts. We show that the crater statistics admit two contradictory age ranges for Ida, which may be resolved by other considerations, including the origin and nature of Dactyl. We examine the dynamical constraints on Dactyl (Petit *et al.* 1994) that imply a low mass density of Ida. Finally, we consider the implications of all these dynamical and compositional constraints, including the observed colors of Ida and Dactyl, for the original formation from the Koronis parent body.

II. CRATER STATISTICS

The cumulative size–frequency distribution for craters is shown in Fig. 1. The solid curves show crater counts for Gaspra and Ida reported by Belton *et al.* (1992 and 1994, respectively), with dashed lines to the left showing extrapolations down to about 100 m, where values are approximately equal. The extension up to 4 km diameter for Gaspra is based on the interpretation of large concavities as craters by Greenberg *et al.* (1994).

For Ida, we add counts up to $\sim$15 km diameter, as shown in Fig. 1. Some of these very large craters were identified by Belton *et al.* (1994), but were not included in the statistics presented there. A key to the ten features we identify as large craters is shown in Fig. 2. An additional large concavity (#11 in Fig. 2) does have a strikingly circular appearance in some image frames, but is more likely a feature of the large-scale structural shape of Ida in that region and is not included in our counts. As shown in Fig. 1, in contrast to Gaspra, multi-km craters on Ida follow the same power law as smaller craters.

The size distribution for Ida from 100 m to 4 km (Fig. 1) is strikingly similar to the theoretical distribution obtained by Greenberg *et al.* (1994) for Gaspra (their Fig. 13 curve labeled "cookie-cutter"). In fact, the Ida data fit that theoretical Gaspra curve better than the Gaspra data do. In order to reconcile the theoretical Gaspra distribution with the steeper and more curved Gaspra observational data, Greenberg *et al.* (1994) invoked a crater-erasing im-

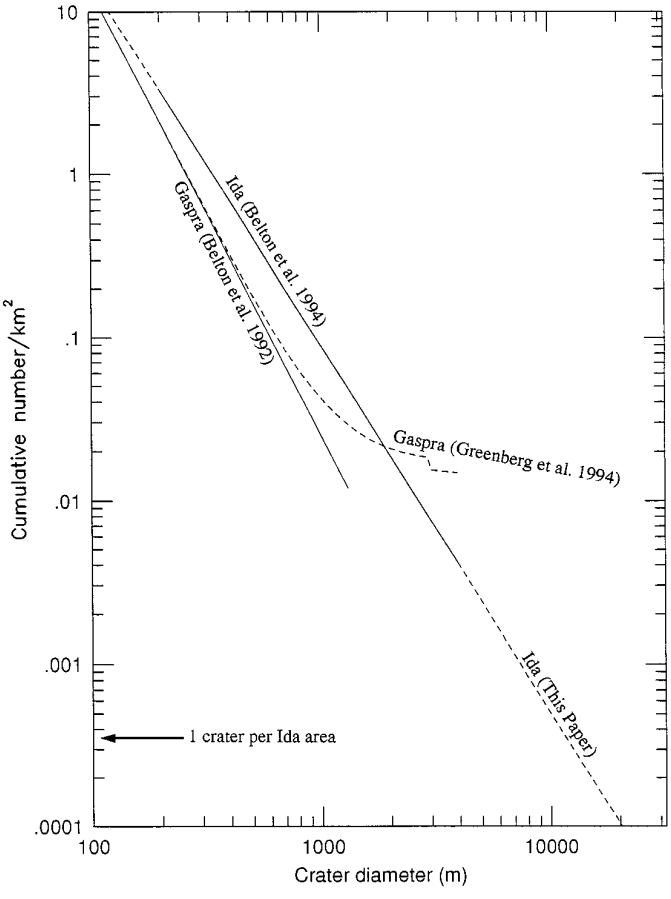

FIG. 1. Crater size–frequency distributions based on the numbers of craters counted on Gaspra and Ida as a function of size from the sources shown. Cumulative number is the number of craters larger than a given diameter. For Ida, multi-km craters follow the same power law as smaller craters. For Gaspra, the distribution curves up for multi-km craters. Extrapolation to smaller sizes (dashed lines to left) shows convergence near 100 m.

pact by a 400 m projectile 50 myr ago, an event expected to occur roughly every 500 myr. An initial hypothesis to explain the Ida data might be that they represent the results predicted by the theoretical size distribution without the slightly *ad hoc* recent big impact. However, as we show below, that simple explanation does not work, because all the processes that determine the expected crater size distribution (production, "jolt erasure," "cookie-cutter" removal, and "sand-blasting") scale differently on Ida than on Gaspra due to the different size of the target.

Those important surface modification processes also render problematic another interpretation of crater statistics. Belton *et al.* (1992, 1994) assumed that craters larger than 1 km represent an essentially unmodified production population on both Gaspra and Ida. For Gaspra, that model led to an age estimate of 200 myr. For Ida, with five times as many craters larger than 1 km (Fig. 1), they estimated an age of 1 byr. However, impact processes have already been shown by Greenberg *et al.* (1994) in the case of Gaspra to erase previously existing craters (even larger than 1 km), as well as produce new ones, so that Gaspra is likely to be ~1 byr old. Similar consideration of the surface effects of collisions is required for interpretation of the impact record on Ida.

III. CRATER PRODUCTION

A. Production Law

Impact crater sizes have generally been related to the sizes of impactors by using scaling laws (e.g., Housen and Holsapple 1990), which extrapolate experimental results via dimensional analysis up to relevant planetary scales. Belton *et al.* (1992, 1994) continue to apply that theoretical approach. Crater sizes can also be modeled using recently developed hydrodynamic numerical simulations of the effects of impacts (Melosh *et al.* 1992, Asphaug 1993). These "hydrocode" models give results significantly different from the scaling laws, especially for large-crater formation on small target bodies. For example, Asphaug and Melosh (1993) showed how a crater as large as Stickney could form on Mars' moon Phobos, an event that seemed impossible according to scaling laws. For Gaspra, hydrocode results showed how a such a small body could survive extremely energetic impacts which leave craters comparable to the size of the asteroid itself, contrary to expectations from scaling laws (Greenberg *et al.* 1994).

Applying the same hydrocode to a larger target (Nolan *et al.* 1993, Nolan 1994) yields the crater production relationship that we adopt in modeling the history of Ida. This relationship indicates the size of a crater produced by an impactor of a given size, striking the target at 3.55 km/sec, which is the mean value for the impacting population according to Bottke *et al.* (1994). In constructing the crater production relationship we assume a spherical target with a volume equal to that of the asteroid.

The hydrocode crater sizes for various size impactors are indicated by triangles in Fig. 3. These results actually show the sizes of the cavities of extreme structural damage, so they represent upper limits to the crater size. In most cases the velocity field for the material shows that nearly all of it is excavated from the crater. However, for the most energetic impacts modeled by the hydrocode (impactors larger than about 50 m in diameter), gravity limits the amount of material than can leave the crater (Nolan 1994), such that final crater size is most accurately constained by gravity-scaling laws. Dashed lines in Fig. 3 show the crater size based on gravity-scaling relationships (from Melosh 1989) for Ida (and for comparison, for Gaspra). Therefore we adopt the crater production law shown by the solid line, following the hydrocode results up to impactors of

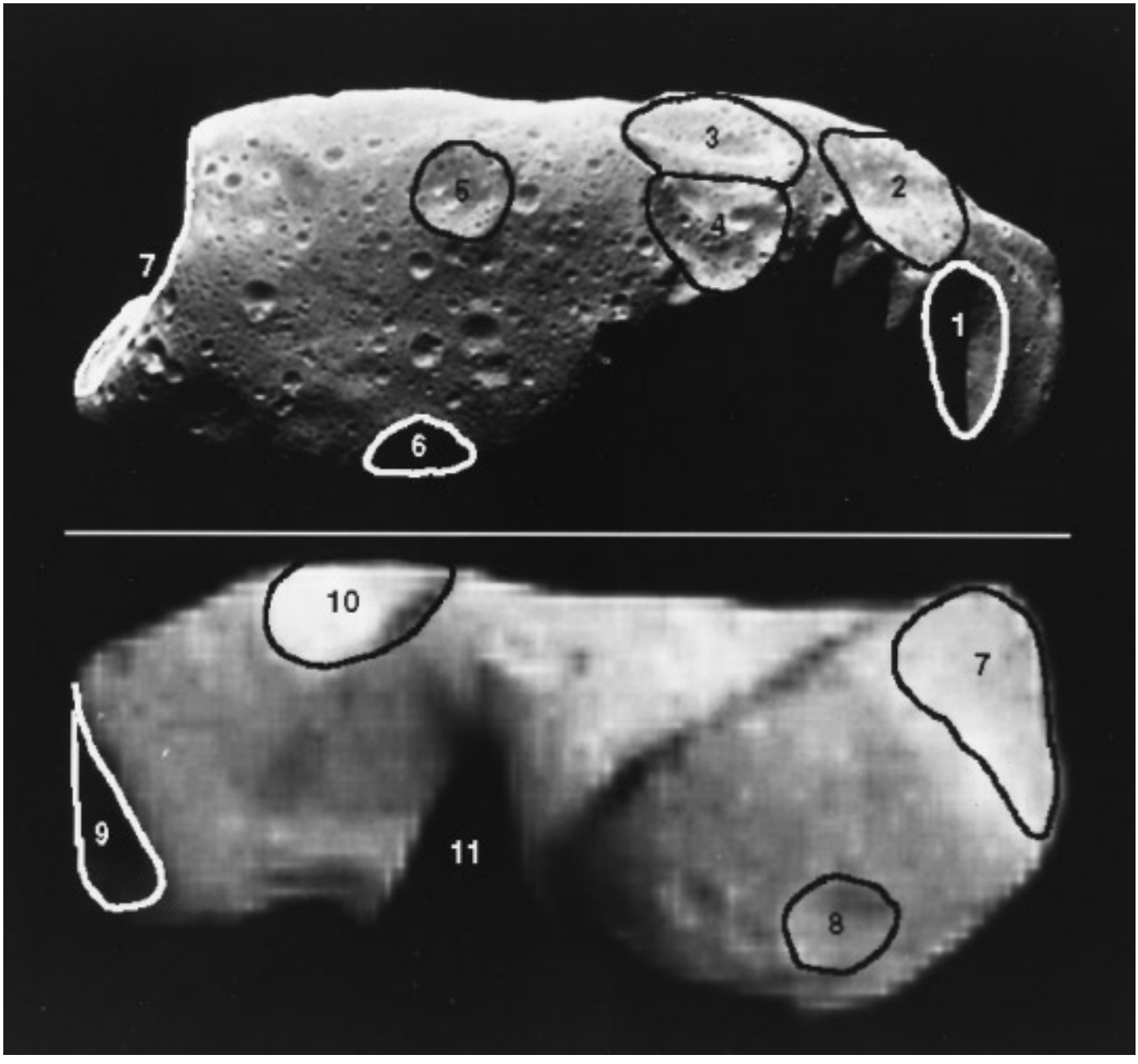

FIG. 2. Key to the 10 largest craters on Ida included in Fig. 1. The depression labeled #11 is not included as an impact crater. Approximate diameters are:

#1 (Mammoth)	~9.6 km
#2 (Lascaux)	~9.9 km
#3 (Undara)	~9.8 km
#4 (no name)	~7.8 km
#5 (Sterkfontein)	~5.3 km
#6 (Postumia)	~6.3 km
#7 (Wien Regio)	~15 km
#8 (Castellana)	~5 km
#9 (Orgnac)	~13 km
#10 (Azzurra)	~7.6 km

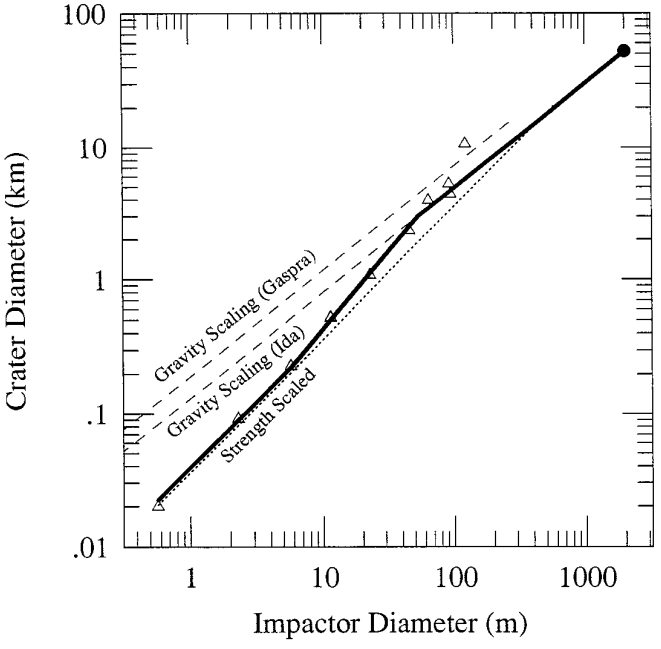

FIG. 3. Crater size produced by a given size impactor hitting Ida at 3.55 km/sec. Triangles show results from hydrocode simulations, with excavation of damaged material limited by the "gravity scaling" line. We adopt the relationship shown by the solid line. For impactors smaller than 6 m diameter, the curve follows a slope of 1, consistent with strength-scaling. For impactors larger than 2 km, the asteroid is destroyed by catastrophic fragmentation; for impactors from 1 km to 2 km global damage is too extensive to leave a crater at the impact site.

50 m diameter and the gravity-scaling limit where it takes over.

Strength scaling, which would be expected to apply for smaller craters, predicts a slope of 1 for the crater production relationship. Such a slope (shown by the dotted line in Fig. 3) fits the hydrocode results well for impactors smaller than about 6 m diameter. For impactors larger than that size, the hydrocode results show a transition from strength-controlled crater scaling with increasingly energetic impacts. This transition had not been successfully predicted by conventional scaling arguments, but is similar to that discovered for Gaspra (Greenberg *et al.* 1994).

The largest impactor that could plausibly leave a concavity recognizable as an impact site is 1 km in diameter, because the resulting crater is already comparable in size to Ida. Thus impacts by projectiles with diameters >1 km do not create craters, but they do erase most preexisting craters by extreme jolting (a process discussed in Section IV). The line in Fig. 3 is extended up to the size of impactor (2 km) above which catastrophic disruption would occur, i.e., most fragments of the target would be ejected at velocities sufficient for escape. This limit is obtained by hydrocode simulations of impact into spheres of diameter 30 km (Nolan *et al.* 1993), Nolan 1994); it is also consistent with the scaling law of Housen *et al.* (1991). Similar simulations with an ellipsoidal target of Ida's dimensions show that it could survive a collision with a projectile larger than 3 km diameter at this velocity, but only if the impact site were near an end of the long axis. Such an event is relatively improbable, so in constructing our scenario for Ida we consider the 2 km projectile to represent the largest survivable hit.

B. Impacting Population

The production law defined by Fig. 3 can be applied to an assumed incoming population of projectiles to obtain a crater production function. We assume that the projectile population is the same as that which best fit the Gaspra crater record in the scenario of Greenberg *et al.* (1994); i.e., the size distribution follows that of the Palomar–Lieden Survey down to asteroid diameter 100 m, and then steepens so that its incremental exponent is −4 for smaller bodies,

$$dn = 2.7 \times 10^{12} D^{-2.95}\, dD \quad \text{for } D > 100 \text{ m}$$
$$dn = 3.4 \times 10^{14} D^{-4}\, dD \quad \text{for } 6 \text{ m} < D < 100 \text{ m},$$

where dn is the number of main-belt asteroids between diameter (in meters) D and $D + dD$. The functions meet and are equal at $D = 100$ m. We cut the distribution at 6 m because there are no cratering data for smaller sizes, and we know the distribution must be less steep for very small bodies to avoid infinite total mass.

If that population bombards Ida for 3 byr according to the intrinsic collision probabilities found by Bottke *et al.* (1994), the statistics of total numbers of craters produced are as shown by the solid curve in Fig. 4. For comparison, the actual crater counts are shown to the same scale as in Fig. 1. The difference of two orders of magnitude indicates that important processes have erased many of the craters that have been created, and/or the surface is much younger than 3 byr.

We can estimate the frequency of disruptive impacts by extrapolating the production curve in Fig. 4 to the right and comparing it with the upper end of the crater production law (Fig. 3), yielding one or two impacts by projectiles larger than 2 km over the 2900 km^2 surface during 3 byr. Thus 3 byr seems a reasonable upper limit to the age of Ida in its current incarnation.

We emphasize that our model assumes that the impacting population is the same one that gave the best fit for Gaspra, and that it has not changed during the lifetime of the surface. It is possible that, for a period of time immediately after the disruption of the Koronis parent body, the population of impactors on Ida was quite different from what it has been since then. Credible modeling of that possibility would be a great challenge, given the current state of understanding of processes of large-body

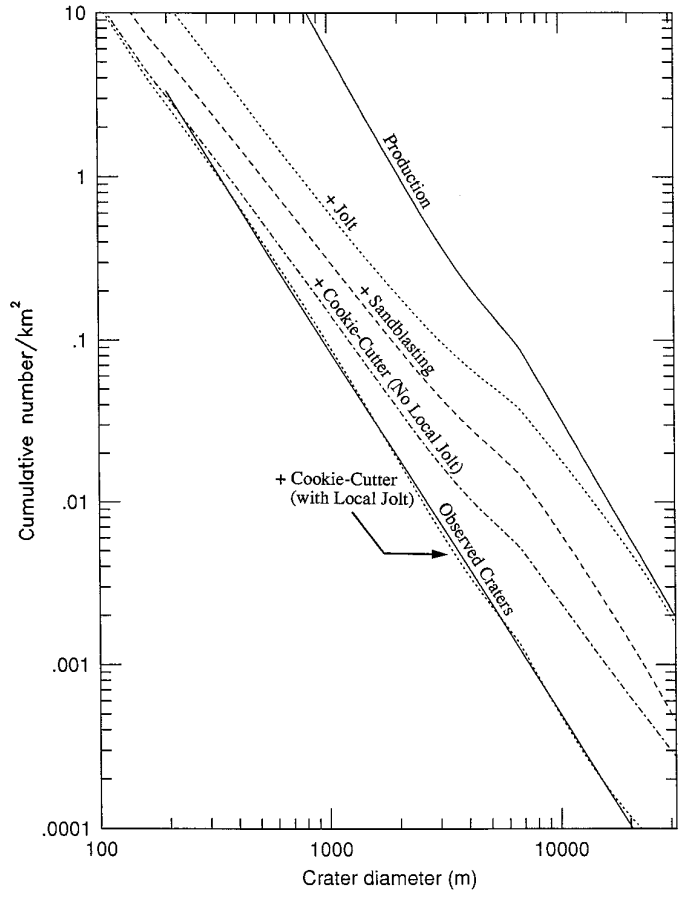

FIG. 4. Theoretical crater size distribution for craters produced over 3 byr, and for the number expected to remain on the surface after the various removal processes are taken into account. The curves include successively more processes going down the page (e.g., the line labeled "+Sandblasting" includes Production + Jolt + Sandblasting). The straight solid line represents the size distribution observed on Ida (from Fig. 1). The lowest dashed line (near the solid line) includes all production and erasure processes considered here; it represents the steady-state equilibrium distribution at 3 byr, i.e., with no major impacts either overdue or having occurred recently.

(Koronis parent) disruption. However, if the surface proves to be old enough so that crater production and erasure are in equilibrium (which holds for an age >1 byr as shown in Section IV), any record of anomalous early bombardment would have been erased by subsequent saturation cratering.

It is also plausible that the steep size–frequency distribution that we have assumed for the impacting population smaller than 100 m is relatively recent. This distribution is not consistent with the expected equilibrium for a collisionally evolved population (Dohnanyi 1969), so it might represent the product of a recent large disruption event. In fact this part of the population would be expected to come to equilibrium in about 50 myr, i.e., equal to the lifetime of a 100 m body (Greenberg and Nolan 1989, Durda 1993). Preliminary study of this possibility suggests that even if the impacting population had been near equilibrium before 50 myr ago, our conclusions (Sections IV and V) about the age of the surface based on the current crater statistics would remain unchanged.

IV. CRATER ERASURE PROCESSES

A. Jolting the Surface

Greenberg *et al.* (1994) introduced global jolting of an asteroid's surface as a critical process governing the observed crater size distribution. As shown by Nolan's hydrocode simulations of impacts, an impact great enough to create a crater of a few km diameter, or greater, causes material over the entire surface to jump up and fall back, largely destroying topography of a scale that increases with the impact energy, as shown in Fig. 5. For example, on Ida, an impact that creates a 10 km diameter crater will simultaneously destroy all craters smaller than 100 m. Figure 5 also shows the similar relationship for Gaspra for comparison. (The Gaspra curve has been improved slightly by refinements in the hydrocode analysis since Greenberg *et al.* 1994, but it has not changed enough to significantly affect that work.) On Gaspra, formation of a given size crater results in destruction of much more topography than on Ida, due to the smaller size of the target.

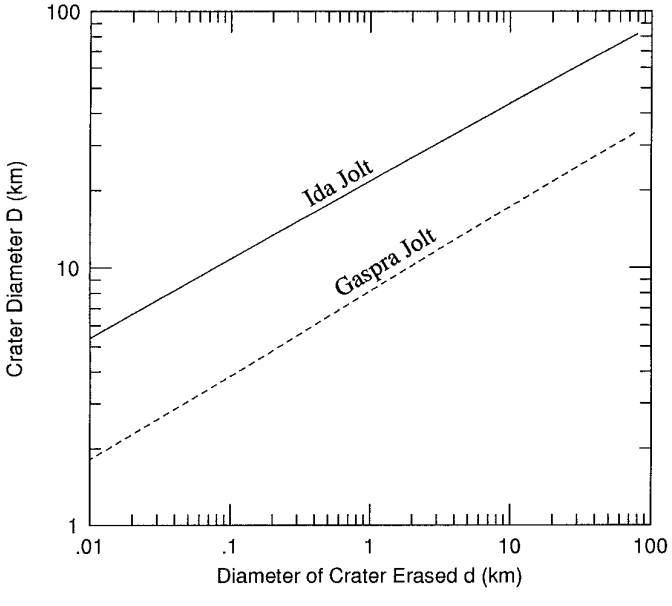

FIG. 5. An impact that creates a crater of a size shown on the ordinate also removes by seismic shaking ("jolts") all craters on the asteroid smaller than indicated on the abscissa. Projectiles larger than 1 km in diameter (which create 30 km craters) may not actually create recognizable craters, but no craters are large enough to be safe from erasure by jolt from such giant impacts.

The hydrocode models produce surface jolting even if the surface is solid rock, because the shock wave generated by the impact fragments surface material. Even during this process, in an irregularly shaped asteroid, it is plausible that large interior blocks might remain unfractured because the shock would not advance uniformly through the interior, and because internal reflections of seismic waves would superpose in an irregular pattern.

The effect of periodic erasure of smaller craters, superimposed over on-going production is shown in Fig. 4 by the line labeled "jolt." This curve would predict the observed crater statistics after 3 byr, if there were no other crater removal processes in effect.

B. Sandblasting

While jolt is a process by which large-crater formation erases smaller craters, the cumulative effect of smaller craters can erase larger ones as well, a process analogous to industrial sandblasting. Sullivan *et al.* (1996) describe evidence for this process in the morphology of eroded craters on Ida. In order to model this effect, we assume that an existing crater is eliminated if the surface is then saturated three times over by craters with diameters between 10% and 100% of its own. In other words, the lifetime of a crater is limited by the time it takes for the total area of craters produced in that size range to reach three times the target area. This algorithm is based on a model in which craters smaller than 10% of the size of the target crater are assumed to only soften its appearance, while impacts in the included range can destroy morphological structure enough to make it unrecognizable.

This sandblasting was a negligible process in the case of Gaspra, where jolting erases craters on such a short time scale that sandblasting effects never accrue. In fact we have applied the same algorithm described here to the case of Gaspra, and it has no significant effect.

If we include sandblasting as well as jolting, the crater size distribution is moved down to the curve labeled "sandblasting" in Fig. 4, now much closer to the actual observed craters on Ida.

C. The Cookie-Cutter Effect

Formation of a crater eliminates all smaller craters at its impact site. This process cuts circular holes in the surface distribution of craters, like a cookie cutter removing dough. We first consider an assumption that any smaller crater is destroyed (rendered uncountable) if its center is within one radius of the center of the newly formed crater, i.e., the obliteration factor (defined by Greenberg *et al.* 1994) is $C = 1$. The effect on the distribution is shown by the curve labeled "cookie cutter" in Fig. 4. This combination of production modified by jolting, sandblasting, and the cookie-cutter gives numbers of craters similar to those at the small end of the observed size range. However, the slope of the distribution is too shallow, so there is an excess of multi-km craters in this simple model.

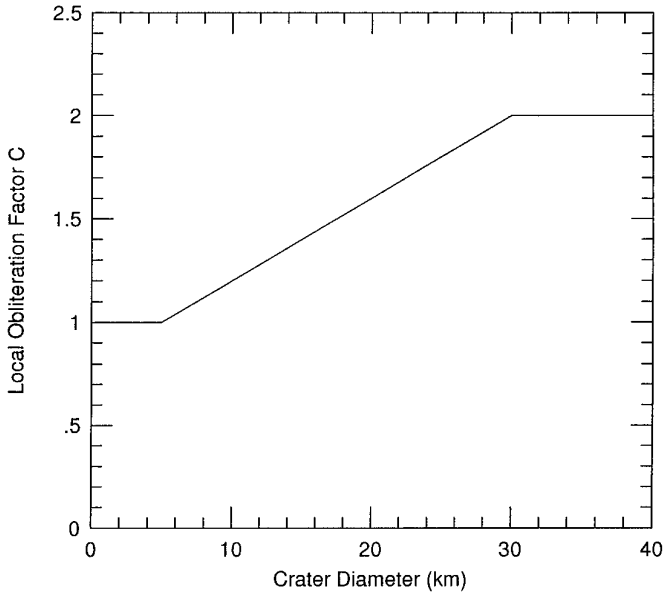

FIG. 6. In the model presented here, a large crater (diameter > 30 km) destroys all topography (including preexisting craters) out to twice the crater's radius ($C = 2$), while craters smaller than 5 km only destroy features within their own radius ($C = 1$).

A more complete cookie-cutter algorithm takes into account that local jolt and crater ejecta can erase a region somewhat beyong the rim of a new crater. Sullivan *et al.* (1996) describe evidence for seismic shaking of local regions around large impact craters, based on regolith maturity inferred from surface color. Hydrocode simulations (Nolan 1994) suggest a general increase in the obliteration factor for multi-km craters, although they do not define a precise relationship. We adopt the obliteration factors shown in Fig. 6 (e.g., a crater larger than 10 km destroys all smaller craters out to 1.2 radii from its center), which are somewhat arbitrary, but are consistent with the hydrocode experiments and with qualitative geological interpretation. Inclusion of this more realistic algorithm for the cookie-cutter gives the lowest theoretical curve in Fig. 4 ("cookie-cutter with local jolt"), which agrees quite well with observations of Ida.

Based on this result alone, the cratering record seems consistent with an age of 3 byr for the surface of Ida, not necessarily as short as the 1 byr value estimated by Belton *et al.* (1994). The difference is due to our approach of modeling the impact processes (crater forming and erasing) on an Ida-sized body, rather than relying on comparisons with impact records on othe cratered planets. However, constraints other than the cratering record to rule out older ages. As discussed in Section I, the tightest such constraint remains Durda's (1994) estimate of $<\sim 1.5$ byr.

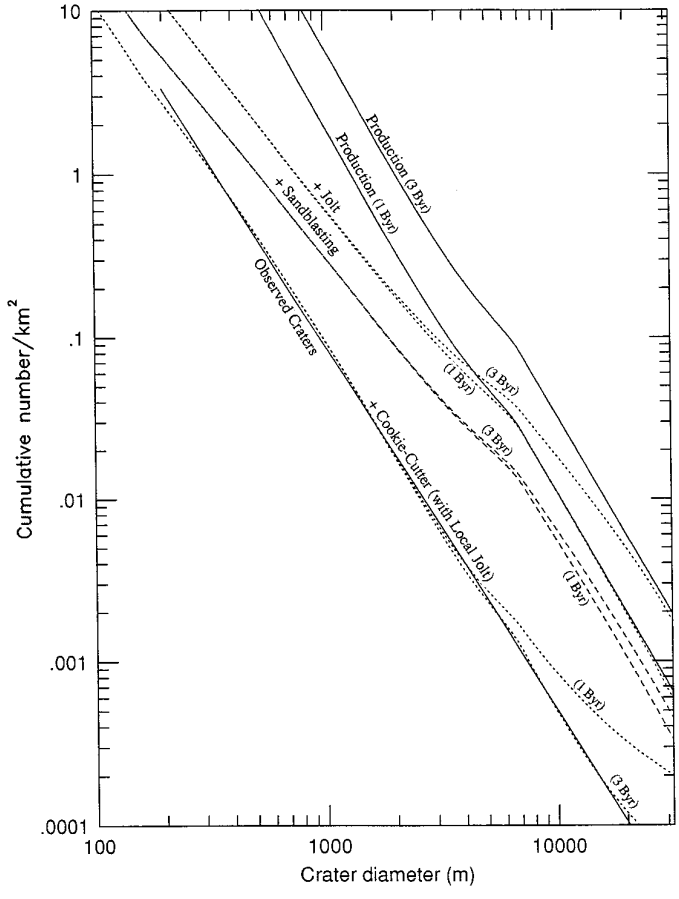

FIG. 7. Similar to Fig. 4, except that size distributions for an assumed age of 1 byr are compared with those for 3 byr.

V. A MORE YOUTHFUL IDA

In order to explore whether younger ages for Ida's surface might be consistent with the impact record, we computed theoretical crater size distributions based on the same production and erasure processes as discussed above (including the local jolt effect of Fig. 6), but assuming ages. Figure 7 shows the crater distribution expected 1 byr after starting with an initial *tabula rasa*. By definition, the production curve is a factor of 3 lower than the 3 byr case. However, Fig. 7 shows that the various erasure processes reduce the numbers to nearly the same as in the 3 byr case, again closely matching the observed counts. In other words, after 1 byr the surface is essentially saturated with craters over the range from 200 m to 4 km; over that crater size range further production is in equilibrium with erasure, so that the counts do not change between 1 and 3 byr.

However, for craters above 4 km in diameter, the theoretical curve for a 1 byr age diverges from that for the 3 byr age. At larger crater sizes, there are more craters at 1 byr than at 3 byr, despite the fact that there have only been one third as many produced. The reason that numbers of craters decrease with time between 1 byr and 3 byr is that erasure (or, equivalently, extreme degradation) of these larger craters can only be done by the most energetic possible impacts, which generally do not occur until after 1 byr.

In comparison with the actual Ida crater counts, the expected crater statistics for any age between 1 byr and 3 byr fit well for craters from 200 m to 4 km. For larger craters, the 3 byr theoretical curve matches the observations closely. The 1 byr curve is off by a factor of 2, but given uncertainties in statistics for multi-km craters, this fit is acceptable. Therefore, our crater formation and destruction scenario is consistent with Durda's independent constraint on the Koronis family's age.

We next compare crater statistics expected at various ages of Ida (Fig. 8), continuing our discussion in order of decreasing age. At 500 myr the trend that was seen in comparing 1 byr with 3 byr continues with an even greater divergence from observed numbers of large craters (by a factor of 3) extending even further (down to craters of

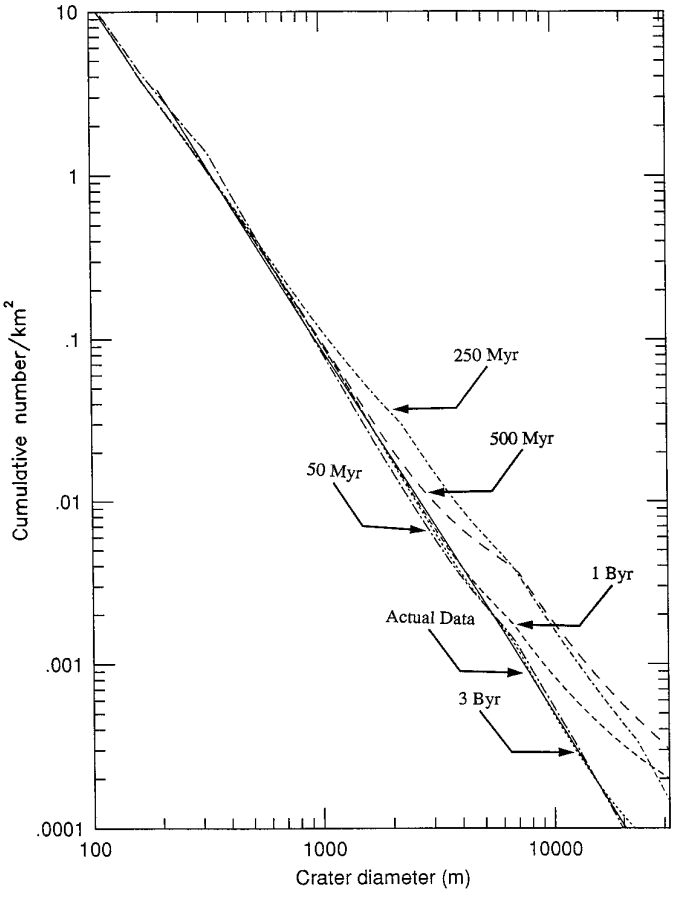

FIG. 8. Expected crater size distributions for a range of ages of Ida's surface. At 50 myr, the theoretical curve fits the observed distribution. For an older surface (up to nearly 1 byr), the expected numbers of craters are higher. But after 1 byr, removal processes reduce the numbers to a steady state near the observed distribution.

~3 km), for the same reason as a 1 byr, but more so. At an age of 250 myr, the mismatch extends from the largest craters down to 1 km. However, at 250 myr the discrepancy is never by more than a factor of 2, because of the very small crater production at this young age. In fact, at an age of only 50 myr (Fig. 8), the production curve for craters larger than 1 km is down to the level of the actual observed counts, so the theoretical crater statistics match observations at all sizes.

It may seem paradoxical that as age increases from 250 myr to 1 byr the number of intermediate-sized craters decreases back to the level at 50 myr. However, this result is reasonable because the increasing numbers of larger impacts tend to destroy craters in the 1–10 km size range until equilibrium is reached after about 1 byr. The size distributions computed here assume that no infrequent impacts have occurred at anomalous times, e.g., that no large impacts are either overdue or have happened more recently than their average frequency. Thus the curve for 50 myr is based on an assumption that no anomalous large impacts with mean frequencies of greater than 50 myr have occurred. The curves for >1 byr represent average conditions in the steady state, not necessarily the actual condition at any given time. For example, an anomalously recent large impact might temporarily lower the numbers of smaller bodies or if large impacts are coming due, the numbers of small craters might temporarily increase above the equilibrium. In such disequilibrium states, the size distribution would generally not be straight on these plots. In fact such a condition, due to an anomalous recent impact, was required to explain the Gaspra crater-size statistics (Greenberg *et al.* 1994). Although even after 1 byr Ida might often differ from the solution shown, the observed size-distribution can only match the model distribution at ages >1 byr or near 50 myr.

Therefore it appears our model can match observed crater statistics for a surface age >1 byr (when crater numbers are in a steady state) or about 50 myr (when crater production still dominates). We can eliminate ages >1.5 byr based on Durda's analysis. Next we consider potential ways to discriminate between an age of 50 myr on one hand and >1 byr on the other.

One approach is to consider morphology and general appearance of the craters on Ida. Belton *et al.* (1994) find that about 60% of craters larger than 1 km appear ''degraded'' (80% for craters >2 km). Belton *et al*. suggest that the substantial portion of degraded craters implies that the system has reached saturation of craters, i.e., a steady state between production and removal. If that interpretation is correct, it would rule out the age near 50 myr, for which our models shows crater statistics to be dominated by production (Fig. 8). At 50 myr, removal processes have not had time to play a big role, but after 1 byr the crater population has achieved a steady state, which would be consistent with Belton *et al*.'s interpretation.

If the 50 myr age is to be defended at all, a case would need to be made showing that the steep size distribution of impactors could extend down to sub-meter scale and account for the observed crater degradation in that short amount of time. Another line of evidence that supports the 50 myr age comes from the existence of the satellite Dactyl (see Sec. Ic). The most plausible origin for Dactyl is a part of the same event that produced Ida, and it is unlikely that Dactyl can survive catastrophic impact longer than 100 myr. In Section VI we discuss the implications of Dactyl for the history of the Ida/Dactyl system.

VI. IMPLICATIONS OF DACTYL

A. Lifetime of Dactyl

The lifetime of Dactyl can be read from Fig. 7 in the following way. Impacts that create craters of about 1 km diameter on Ida would marginally destroy Dactyl (diameter 1.5 km). Fig. 7 shows that ~2 such events occur in 1 byr on a target area of 1 km^2. Dactyl's area is about 8 km^2, part of which at any time is protected from impact by the collisional shadow of Ida. Therefore, a disrupting impact is expected in $\sim 10^8$ yr. If one assumes that Dactyl formed as a satellite at the same time as the formation of Ida, the Koronis parent must have broken up only about 100 myr ago. Durda's (1993) calculation of the age of the Koronis family does allow such a young age if the parent body was near the small end of possible sizes (diameter > 110 km, according to Zappalà *et al.* 1984). The surface of Ida must be of the same age, consistent with our value of 50 myr (Section V), not >1 byr.

An age of Ida >1 byr seems to require that Dactyl formed long after Ida. That hypothesis is difficult to support because, as discussed in Section VII, formation along with Ida seems to be the most plausible model; persuasive models of origin by capture or by ejection from Ida have not yet been constructed. Nevertheless, there may be ways to reconcile the most likely cratering history (Ida's surface age >1 byr) with the most plausible satellite formation mechanism (accompanying Ida's formation). Perhaps a satellite did form along with Ida, but was disrupted (perhaps several times), after which a large fragment, or a reaccumulation of fragments, formed the current satellite. A significant portion of the debris from the disruption would have had to have been ejected at less than 2 m/sec to avoid capture by Ida or escape. Further study of disruption processes may shed light on the plausibility of this hypothesis.

Another possibility is that Dactyl has been gradually, but significantly, eroded as crater ejecta escaped the satellite during the past 100 myr, so that during most of that time it was large enough to resist disruption by the largest im-

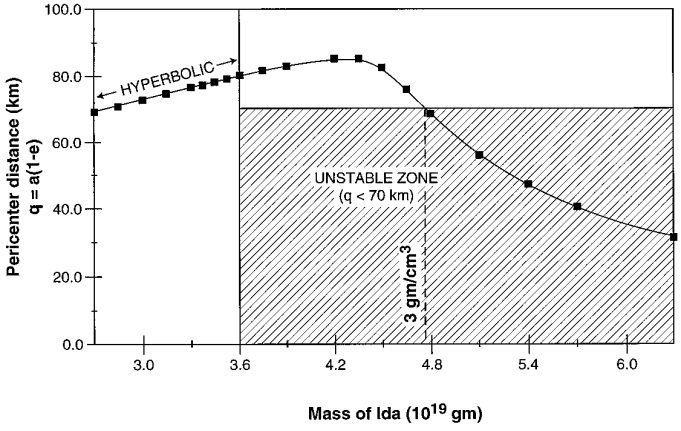

FIG. 9. A wide range of Keplerian orbits fit the arc of motion observed during the Galileo encounter, each corresponding to a given assumed mass for Ida. The squares show the pericenter distance q as a function of Ida's mass (Byrnes and D'Amario 1994). Orbits with $q < 70$ km would be unstable, so the mass of Ida is less than about 4.8×10^{19} gm, which corresponds to a density of Ida <3 gm/cm^3 for a volume of 16,000 km^2.

pactor to have hit it. In that case Dactyl may be much older than its current 100 myr life expectancy. This scenario, along with other considerations of the fate of ejecta from Dactyl, is explored in more detail by Geissler *et al.* (1996).

B. Orbit

Dactyl's orbit also places important constraints on the nature and history of the Ida system. Galileo images of Dactyl over the duration of the encounter have permitted a fit to possible orbits (Byrnes and D'Amario 1994, Belton *et al.* 1995). Acceptable orbits lie close to a one-dimensional line in orbital *a, e, i* space: The semi-major axis a might have any value greater than 40 km, but each a value has a corresponding value of the orbital eccentricity. All candidate orbits have inclination i well constrained (because the Galileo camera was near the orbital plane) near 10° relative to prograde equatorial motion. (By prograde we mean in the same direction as Ida's rotation; note however that Ida's rotation is retrograde relative to the ecliptic.) Each candidate orbit also corresponds to a particular assumed mass for Ida, as shown in Fig. 9.

We have examined the stability of a wide range of hypothetical orbits for objects orbiting Ida, by numerically integrating the motion. Ida has been modeled as a triaxial ellipsoid, as a pair of contacting spheres with a massless cylinder filling the space between them, and with a geometry similar to that reported by Thomas *et al.* (1996) for the real Ida. Results are similar for all those cases; the specific cases summarized here are based on the triaxial-ellipsoid model. In general, retrograd orbits are stable and long-lived even if their pericenter distances $q \equiv a(1 - e)$ are as small as 50 km. We have also discovered classes of commensurable retrograde orbits with even lower values of q. Stable prograde orbits are possible only in a more limited range. Prograde orbits with pericenter $q < 70$ km generally escape from or collide with Ida within a few days. This numerical study of orbital stability was described by Petit *et al.* (1994). (Applications of the same software to the dynamics of impact ejecta near Ida are discussed by Geissler *et al.* (1994a,b,c, 1996)).

The boundary for stable prograde orbits is shown on Fig. 9 for comparison with the candidate orbits obtained by Byrnes and D'Amario (1994). Our numerical experiments included tests of the specific range of elliptical orbits proposed by Byrnes and D'Amario. In that set of orbits the general rule is confirmed: All orbits with $q < 70$ km impacted Ida or escaped in only a few hours. The orbits with larger values of q are found to be stable for at least 10^7 sec, which corresponds to hundreds of orbital periods.

Because each candidate orbit corresponds to a particular assumed mass for Ida, our limit on q provides an upper limit on Ida's mass of 4.8×10^{19} g. Combined with estimates of Ida's volume (Thomas *et al.* 1996), this result implies a maximum density of about 3 g/cm^3, and probably significantly less (Belton *et al.* 1995). Interestingly, Farinella *et al.* (1981) had much earlier predicted that such a body might have density in this range.

If Ida were of ordinary chondritic composition (density about 3.6 g/cm^3), it would need to have a porosity >20% to account for its low bulk density. Belton *et al.* (1995) also consider a composition with high nickel–iron content (like iron or stony-iron meteorities). Presumably, as for meteorites, such a composition would result if Ida's parent body had been differentiated and Ida inherited a disproportionate share of the densest component. In that case, to meet the bulk density constraint would require very high porosity, so Belton *et al.* (1995) favor a stony composition with a chondritic amount of metal. We consider additional possibilities. On one hand, although compositions similar to iron or stony iron are ruled out by the above argument, it is still possible to have substantial enhancement of the iron component above chondritic quantities without requiring implausible porosity. On the other hand, if the Ida/Koronis parent (diameter >110 km) had in fact been differentiated, a sample of Ida's size is more likely to represent mantle material than the relatively small volume of iron in a core. In that case the material density would be near 3 g/cm^3, predominantly olivine, even with no porosity. If the sample included crustal material (~2.7 g/cm^3), its density would be even less. Therefore, we conclude that a plausible model for Ida's composition has no metallic component or considerably less than the chondritic value. This model is discussed further in Section VII.

VII. ORIGIN OF IDA AND DACTYL

As a member of the Koronis family, Ida is widely assumed to have formed from the disruption of the Koronis parent body. Durda (1994, 1996) has explored the dynamics of formation of gravitationally bound fragments. He models a distribution of fragments with a power-law size distribution moving outward from the disrupted body. A variety of assumptions about the initial spatial and velocity distribution were tested, all within the range of conventionally assumed models of catastrophic disruption. In order to be conservative, Durda avoided models in which local initial conditions would favor clustering of material. Nevertheless, in any disruption event ~1% of the fragments of any given size are members of bound pairs of bodies. Much less frequently, groups of three or more fragments are gravitationally bound.

For about 50–70% of the bound pairs, the components collide with one another, usually at speeds less than a few 10's of m/sec. In that case, the components would suffer some damage at the contact point and either come to rest as a contact conglomerate structure, or bounce apart only to join together upon subsequent impact. In other cases, the components remain in mutual orbit like Ida and Dactyl.

These results frequently produce objects with basic characteristics similar to Ida. The general shape of Ida suggests an underlying structure dominated by two or three large structural components, which may represent gravitationally bound fragments that have reaccumulated. Dactyl is likely to be a fragment that remained bound but was not reaccreted.

In the cases explored by Durda, components of most bound pairs or groups originated along a roughly radial set of source positions within their parent body. Fragments that originate at different angular positions within the parent body (i.e., different latitudes or longitudes) diverge too quickly to remain gravitationally bound to one another.

Further information on the source locations within the Koronis parent body comes from the composition of Ida and Dactyl inferred from spectral information and the density constraint (Section VI). Data from Galileo are preliminary due to complex issues of calibration and interpretation of sampling in wavelength. They do indicate a spectrum for Ida that is consistent with chondritic (i.e., undifferentiated) composition, but we will discuss an alternative interpretation.

The imaging camera shows that for most of Ida's surface, there is a gradual rise in reflectivity from the violet to 1 μm, with a local minimum near 1 μm, which for rocky materials usually represents an absorption band due to pyroxene. The general increasing trend continues up to 5 μm according to preliminary results from Galileo's Near-Infrared Mapping Spectrometer (Carlson *et al.* 1994, Granahan *et al.* 1994). Some parts of Ida's surface appear more blue; specifically, in these regions the spectrum from blue to red is relatively flat and the minimum near 1 μm is slightly deeper. At longer wavelengths these ''blue'' regions are indistinguishable from the rest of Ida. Such blue regions have often been interpreted as representing ''less mature'' regolith in various planetary contexts, including the discussion of Ida's geology by Sullivan *et al.* (1996). Geissler *et al.* (1996) show how emplacement of such less mature regolith may be mapped back dynamically to a specific source, the crater Azzurra.

Dactyl looks different spectrally from both the red and blue regions of Ida. The satellite is similar to the predominant (less blue) regions of Ida over visible wavelengths, but has a much deeper 1 μm band. The Dactyl spectrum then parallels Ida's up to about 5 μm, except for a slight dip relative to Ida at about 2.3 μm (Carlson *et al.* 1994, Granahan *et al.* 1994).

While it may be possible to construct a model of Dactyl in which the satellite has the same composition as Ida, with surface grain size tuned to give the observed spectral structure, such a model would seem rather contrived. In contrast, the spectral features that distinguish Dactyl from Ida correspond in position to well-known compositional indicators, offering a more natural explanation. The nature of the 1 μm band for Dactyl can be interpreted as enrichment in either olivine or pyroxene relative to Ida. The dip at 2.3 μm corresponds to another pyroxene band, suggesting enrichment in that mineral specifically (Carlson *et al.* 1994). Independent of whether the differences in spectra between Ida and Dactyl are predominantly due to olivine or pyroxene, the implied difference in composition indicates that there was some degree of differentiation in the Koronis parent body.

Consider a differentiated parent body with diameter ~150 km, and with metallic nickel-iron concentrated to some degree toward the center, and low density materials (pyroxene) near the structure (Fig. 10). If we were to carve out an Ida-sized fragment (or fragments) at random, the chance that it would include much metal is small. Surely it would be improbable to sample just enough core to obtain a chondritic complement of metal. Most likely the sample would be depleted in metal, and consistent with the low density we infer from Dactyl's orbit (Section VI). Ida is most likely a sample of the parent body's olivine mantle (~90% of the volume of a differented chondrite), with enough pyroxene (either undifferentiated from the mantle or sampled as part of the crust) to appear ''chondritic.''

If Dactyl was created according to Durda's model, it must have formed either deeper in the parent than the Ida material (more pure olivine from the deep mantle) or close to the surface (sampling pyroxene). Either of these compositions would be consistent with the spectral differences between Dactyl and Ida, although if the 2.3 μm feature in

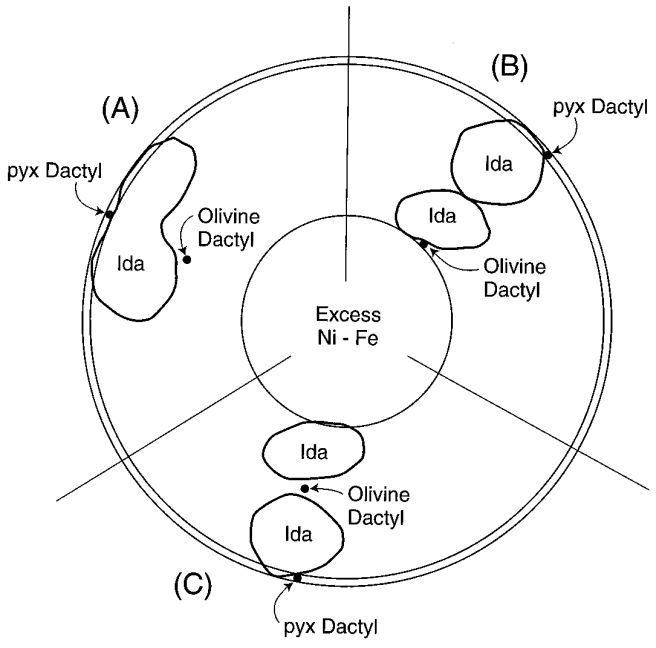

FIG. 10. Dynamical constraints on binary formation during parent-body disruption, plus compositional information inferred from spectral data place constraints on the source of Ida and Dactyl in the Koronis parent. The significant compositional difference between Dactyl and Ida implies that the parent was at least somewhat differentiated. Here for illustration we show a completely differentiated parent body, but similar implications could be drawn if the parent were only partially differentiated. These models are not intended to be definitive, but rather to illustrate the importance of synthesizing physical, dynamical, and compositional information. (A) Ida is most likely to sample predominantly the olivine mantle, but must include the crust to account for its pyroxene component. Dactyl (which contains either more olivine or more pyroxene than Ida) probably came from a site radially aligned with Ida, either deeper in the mantle (olivine) or at the surface (pyroxene). (B) If Ida is a contact binary, its components were originally radially aligned, with one sampling the pyroxene, and with Dactyl either deeper in the olivine mantle or at the pyroxene surface. (C) It is also possible that an olivine Dactyl comes from a site between major components blocks of Ida.

Dactyl's spectrum proves to be real, it would argue strongly for Dactyl's origin near the surface of the parent planet. It may also be possible to construct models based on partial or local differentiation.

VIII. CONCLUSIONS

Collisional and dynamical processes are central to nearly all of the observable properties of the Ida/Dactyl system. Dactyl's orbit places a meaningful constraint on Ida's density. Combined with spectral information about the colors of Ida and Dactyl, and dynamical models of satellite formation, the density helps us develop preliminary models of the source of these bodies in the Koronis parent body.

Investigation of orbital motion in the gravitational field of this odd-shaped, rapidly rotating body also provides explanations of a variety of important observations and processes as described by Geissler *et al.* (1996). These studies show how ejecta trajectories may have governed the distribution of material over the surface, including global erosion, transport of material between Ida and Dactyl (Geissler *et al.* 1994c), and emplacement of the large boulders (Geissler *et al.* 1994a,b) and the variously colored units or regolith discovered in Galieleo images.

Combining models of the physical processes of crater formation and removal by impacts with actual crater statistics on Ida suggests that Ida's surface is either ~50 myr old or >1 byr old. The existence of Dactyl, which probably formed with Ida and which currently has a life expectancy of only 100 myr, seems to argue in favor of the younger age. However, Dactyl may be the most recent incarnation of an earlier satellite that has eroded, or disrupted and reaccreted, to its current size. In that case Dactyl's existence could be consistent with an age >1 byr. The degraded condition of many craters also qualitatively argues for an older age (Belton *et al.* 1994), unless the population of inpactors is dominated by small particles. All these constraints are consistent with the upper limit of about 1.5 byr on Ida's age (Durda 1993), based on the collisional history of the Koronis family.

Any reconstruction of the source of Ida and Dactyl must synthesize dynamical and physical constraints with compositional information. Such a synthesis based on current understanding suggests that Ida's parent body was substantially (but not necessarily completely) differentiated, such that Ida is depleted in iron, and that Dactyl sampled a compositionally different region in the parent body. Continuing interdisciplinary approaches are needed to test this model further.

ACKNOWLEDGMENTS

This work was made possible by Professor Greenberg's participation on the Imaging Team of the NASA/JPL Galileo mission. We are grateful to the members of the Imaging Team, led by Dr. M. Belton, for comments and critiques on this specific work, and for providing a stimulating intellectual setting for the analysis of Galileo data. We thank all members of the Galileo project for their contributions to obtaining the magnificent imagery returned by the spacecraft. Careful reviews of the manuscript by Paolo Paolicchi and Eileen Ryan led to considerable improvements. Data processing for the work reported here was managed by Joe Plassmann. Undergraduate assistant Terry Hurford helped with the analysis of orbital stability for Dactyl. Much of the analysis reported here was supported by a grant from NASA's Planetary Geology and Geophysics program.

REFERENCES

ASPHAUG, E., AND H. J. MELOSH 1993. The Stickney impact on Phobos: A dynamical model. *Icarus* **101,** 144–164.

ASPHAUG, E. (1993). *Dynamic Fragmentation in the Solar System.* Ph.D. Thesis, Univ. of Arizona.

ASPHAUG, E., J. M. MOORE, D. MORRISON, W. BENZ, M. C. NOLAN, AND

R. J. Sullivan 1996. Mechanical and geological effects of impact cratering on Ida. *Icarus* **120,** 158–184.

Belton, M. J. S., J. Veverka, P. Thomas, P. Helfenstein, D. Simonelli, C. Chapman, M. E. Davies, R. Greeley, J. Head, S. Murchie, K. Klaasen, T. V. Johnson, A. McEwen, D. Morrison, G. Neukum, F. Fanale, C. Anger, M. Carr, and C. Pilcher 1992. Galileo encounter with 951 Gaspra: First pictures of an asteroid. *Science* **257,** 1647–1652.

Belton, M. J. S., C. R. Chapman, J. Veverka, K. P. Klaasen, A. Harch, R. Greeley, R. Greenberg, J. W. Head III, A. McEwen, D. Morrison, P. C. Thomas, M. E. Davies, M. H. Carr, G. Neukum, F. P. Fanale, D. R. Davis, C. Anger, P. J. Gierasch, A. P. Ingersoll, and C. B. Pilcher 1994. First images of asteroid 243 Ida. *Science* **265,** 1543–1547.

Belton, M. J. S., C. R. Chapman, P. C. Thomas, M. E. Davies, R. Greenberg, K. Klaasen, D. Byrnes, L. D'Amario, S. Synnott, T. V. Johnson, A. McEwen, W. J. Merline, D. R. Davis, J.-M. Petit, A. Storrs, J. Veverka, and B. Zellner 1995. Bulk density of asteroid 243 Ida from the orbit of its satellite Dactyl. *Nature* **374,** 785–788.

Binzel, R. P. 1988. Collisional evolution in the Eos and Koronis asteroid families. *Icarus* **73,** 303–313.

Bottke, W. F., M. C. Nolan, R. Greenberg, and R. Kolvoord 1994. Velocity distributions among colliding asteroids. *Icarus* **107,** 255–268.

Byrnes, D., and L. D'Amario 1994. Report to Galileo Imaging Team, unpublished.

Carlson, R. W., P. R. Weissman, M. Segura, L. W. Kamp, W. D. Smythe, T. V. Johnson, D. L. Matson, F. E. Leader, R. Mehlman, F. P. Fanale, J. C. Granahan, H. H. Keiffer, L. A. Soderblom, and T. B. McCord 1994. Infrared spectroscopy of asteroid 243 Ida and discovery spectra of satellite 1993 (243) 1. *Bull. Am. Astron. Soc.* **26,** 1156.

Durda, D. D. 1993. *The Collisional Evolution of the Asteroid Belt and Its Contribution to the Zodiacal Cloud.* Ph.D. Thesis, Univ. of Florida.

Durda, D. D. 1994. Numerical models of the origin of asteroidal moons during Hirayama family formation. *Bull. Am. Astron. Soc.* **26,** 1158.

Durda, D. D. 1996. The formation of asteroidal satellites in catastrophic collisions. *Icarus* **120,** 212–219.

Dohnanyi, J. 1969. Collisional model of asteroids and their debris. *J. Geophys. Res.* **74,** 2531–2554.

Farinella, P., P. Paolicchi, E. F. Tedesco, and V. Zappalà 1981. Triaxial equilibrium ellipsoids among the asteroids? *Icarus* **46,** 114–123.

Geissler, P., J.-M. Petit, and R. Greenberg 1994a. Ejecta reaccretion on rapidly rotating asteroids: Implications for 243 Ida and 433 Eros. *Proc. Astron. Soc. Pacific*, in press.

Geissler, P., J.-M. Petit, and R. Greenberg 1994b. Ida: Distribution and origin of surface blocks. *Lunar Planet. Sci. Conf.* **25,** 411–412.

Geissler, P., J.-M. Petit, R. Greenberg, W. Bottke, M. Nolan, and D. Durda 1994c. Erosion and regolith redistribution on Ida and its moon. *Bull. Am. Astron. Soc.* **26,** 1157.

Geissler, P., J.-M. Petit, D. Durda, R. Greenberg, W. F. Bottke, M. C. Nolan and J. Moore 1996. Erosion and ejecta reaccretion on 243 Ida and its moon. *Icarus* **120,** 140–157.

Granahan, J. C., F. P. Fanale, R. W. Carlson, L. W. Camp, K. P. Klaasen, M. Belton, C. R. Chapman, A. S. McEwen, and the Galileo NIMS and SSI instrument teams 1994. A Galileo multi-instrument spectral view of 243 Ida and 1993 (243) 1. *Bull. Am. Astron. Soc.* **26,** 1156.

Greenberg, R., M. C. Nolan, W. F. Bottke, and R. Kolvoord 1994. Collisional history of Gaspra. *Icarus* **107,** 84–97.

Greenberg, R., and M. C. Nolan 1989. Delivery of asteroids and meteorites to the inner solar system. In *Asteroids II*, pp. 778–804. Univ. Arizona Press.

Housen, K. R., and K. A. Holsapple 1990. On the fragmentation of asteroids and planetary satellites. *Icarus* **84,** 226–253.

Housen, K. R., R. M. Schmidt, and K. A. Holsapple 1991. Laboratory simulation of large-scale fragmentation events. *Icarus* **94,** 180–190.

Lagerkvist, C. I., A. Harris, and V. Zappalà 1989. Asteroid lightcurve parameters. In *Asteroids II* (R. P. Binzel, T. Gehrels and M. S. Matthews, Eds.) Univ. Arizona Press, Tucson, pp. 1162–1179.

Marzari, F., D. Davis, and V. Vanzani 1995. Collisional evolution of asteroid families. *Icarus* **113,** 168–187.

Melosh, H. J. 1989. *Impact Cratering: A Geologic Process.* Oxford Univ. Press, New York.

Melosh H. J., E. V. Ryan, and E. Asphaug 1992. Dynamic fragmentation in impacts: Hydrocode simulation of laboratory impacts. *J. Geophys. Res.* **97,** 14,735–14,759.

Nolan, M. C., E. Asphaug, and R. Greenberg 1993. Numerical hydrocode modeling of impacts into a body the size of 243 Ida. *Bull. Am. Astron. Soc.* **25,** 1140.

Nolan, M. C. 1994. *Delivery of Meteorites from the Asteroid Belt.* Ph.D. Dissertation, Univ. of Arizona.

Petit, J.-M., R. Greenberg, and P. Geissler 1994. Orbits around a small, highly elongated asteroid: Constraints on Ida's moon. *Bull. Am. Astron. Soc.* **26,** 1157–1158.

Sullivan, R., R. Greeley, R. Pappalardo, E. Asphaug, J. M. Moore, D. Morrison, M. J. S. Belton, M. Carr, C. R. Chapman, P. Geissler, R. Greenberg, J. Granahan, J. W. Head III, R. Kirk, A. McEwen, P. Lee, P. C. Thomas, and J. Veverka 1996. Geology of 243 Ida. *Icarus* **120,** 119–139.

Thomas, P. C., M. J. S. Belton, B. Carcich, C. R. Chapman, M. E. Davies, R. Sullivan, and J. Veverka 1996. The shape of Ida. *Icarus* **120,** 20–32.

Zappalà, V., and A. Cellino 1994. Main-belt asteroids: Present and future inventory. *Proc. Astron. Soc. Pacific,* in press.

Zappalà, V., P. Farinella, Z. Knezevic, and P. Paolicchi 1984. Collisional origin of asteroid families. *Icarus* **59,** 261–285.